A Statistical Framework for Natural Feature Representation

Suresh Kumar, Fabio Ramos, Ben Upcroft and Hugh Durrant-Whyte
ARC Centre of Excellence for Research in Autonomous Systems
Australian Centre for Field Robotics, University of Sydney
NSW 2006, Australia
{*suresh, f.ramos, b.upcroft, hugh*}*@acfr.usyd.edu.au*

***Abstract*— This paper presents a robust stochastic framework for the incorporation of visual observations into conventional estimation, data fusion, navigation and control algorithms. The representation combines Isomap, a non-linear dimensionality reduction algorithm, with Expectation Maximization, a statistical learning scheme. The joint probability distribution of this representation is computed offline based on existing training data.**

The training phase of the algorithm results in a nonlinear and non-Gaussian likelihood model of natural features conditioned on the underlying visual states. This generative model can be used online to instantiate likelihoods corresponding to observed visual features in real-time. The instantiated likelihoods are expressed as a Gaussian Mixture Model and are conveniently integrated within existing non-linear filtering algorithms. Example applications based on real visual data from heterogenous, unstructured environments demonstrate the versatility of the generative models.

***Index Terms*— Feature extraction, Natural feature representation, Statistical learning, Nonlinear manifolds**

I. Introduction

Autonomous navigation and data fusion tasks require robust feature extraction and representation. Traditional schemes in autonomous navigation have focussed on the selection of stable point features through the use of ranging devices (laser [1], sonar [2]). While such techniques have been deployed in unmanned air, ground and underwater vehicles, they do not provide rich characterizations of an unstructured environment in terms of color, texture or other sensory properties.

This paper explicitly focusses on the use of visual observations within autonomous systems to enable rich, probabilistic characterizations of the environment for applications such as feature selection for Simultaneous Localization and Mapping (SLAM), terrain classification and tactical picture compilation.

While the computer vision community has developed several stochastic feature representation schemes, their application in robotics has been limited. Lee et al [3] present a generative visual model based on Independent Components Analysis (ICA) which provides a linear and non-Gaussian framework for feature representation. In the work of Karklin et al [4], a hierarchical probabilistic framework is presented for the detection of higher order statistical structure in natural imagery. A key limitation of these models is that they do not necessarily preserve the inherent similarities in the sensed visual data. Thus multiple observations of the same visual feature may result in different underlying visual states or visually distinct features may possess similar states in these representations. This minimizes their utility in classical estimation and data association tasks. This limitation is addressed here through the application of Isomap [5], a Nonlinear Dimensionality Reduction (NLDR) algorithm that preserves similarities in sensed data according to a user defined distance metric.

This paper explicitly assumes that all visual data (e.g. color, texture) is sampled from the vicinity of a low dimensional manifold embedded in the observation space comprised of raw pixels. In this representation, the visual state of any observation corresponds to the intrinsic coordinates on the manifold. The concepts of NLDR are combined with Expectation Maximization [6] to compute stochastic representations of natural features. Such a representation leads to a compact, nonlinear and non-Gaussian description of high dimensional visual observations such as color and texture. Critically, this representation can be learnt offline and used to infer the underlying states of visual observations in real-time.

Section II presents an overview of NLDR schemes and outlines the basic theory of the Isomap method used in this work. Section III describes the methodology to compute a statistical representation of NLDR algorithms as a mixture of linear models using Expectation Maximization (EM). The statistical representation of natural features results in a *probabilistic likelihood model* that may be integrated within existing non-linear filtering algorithms for state estimation of visual features [7]. The methodology is finally applied to sample imagery acquired by autonomous ground and underwater vehicles. It is demonstrated that this methodology provides a compact, neighborhood preserving, statistical representation of the underlying state of high dimensional visual observations.

II. Nonlinear Dimensionality Reduction

The feature representation scheme presented here is independent of any specific feature extraction algorithm. In this implementation, information theoretic concepts are used to extract features with unique properties within the sensory space. While this feature selection scheme seems ideal for SLAM, task driven feature extractors may be more appropriate in other scenarios.

Each extracted feature is potentially set in a very high dimensional space that is not readily amenable to simple interpretation and reasoning tasks. The development of compact

and useful representations of natural features in unstructured dynamic worlds is critical to the development of next generation autonomous systems. These algorithms have numerous potential applications ranging from data compression, robust data association to assist autonomous navigation and unsupervised feature selection to create terrain models.

While traditional dimensionality reduction methods such as Principal Component Analysis (PCA) and its numerous variants provide theoretically optimal representations from a data-compression standpoint, they are unable to provide neighborhood preserving representations that are crucial to data association. This limitation has motivated the development of various nonlinear embedding methodologies such as Kernel PCA [8], Isomap [5], Laplacian Eigenmaps [9] and Locally Linear Embedding (LLE) [10]. Most NLDR techniques presume that the data lies on or in the vicinity of a low dimensional manifold and attempt to map the high dimensional data into a single low dimensional, global coordinate system. The Isomap algorithm is adopted in this work to provide a low dimensional description of high dimensional features primarily because it estimates the intrinsic dimensionality of the manifold in addition to the underlying states.

A. Theoretical Aspects of the Isomap Method

The Isomap method [5] formulates NLDR as the problem of finding a Euclidean feature space embedding of a set of observations that attempts to explicitly preserve their intrinsic metric structure; the metric structure is quantified as the geodesic distances between the points along the manifold.

The Isomap method assumes that the sensor data $\vec{Z}$ lies on a smooth nonlinear manifold embedded in the high dimensional observation space. It attempts to reconstruct an implicit mapping $f : \vec{Z} \rightarrow \vec{X}$ that transforms the data to a low dimensional Euclidean feature (state) space $\vec{X}$, which optimally preserves the distances between the observations as measured along geodesic paths on the manifold. Significant steps in the Isomap algorithm are summarized next.

B. Nearest Neighbor Computation

Neighboring points on the manifold are determined based on the input space distances $d_z(i,j)$ between pairs of points $i, j \in \vec{Z}$. Each input point is connected to adjacent points based either on the K nearest neighbors or all points within a fixed distance ϵ from the point under consideration. The neighborhood relations are expressed as a weighted graph G over the data points with edges of weight $d_z(i,j)$ between neighboring points.

C. Computation of Geodesic Distances

The length of a path in G is defined as the sum of the link weights along the path. The shortest path lengths d_G^{ij} between two nodes i and j in the graph G are computed through the Floyd's algorithm [11] that generally scales as $O(N^3)$ or the Dijkstra algorithm [12] that scales as $O(N^2 log(N))$, where N is the number of data points.

D. Graph Embedding Through Multi-Dimensional Scaling

Classical Multi-dimensional Scaling (MDS) [13] is now used to compute a graph embedding in k dimensional space that respects closely the geodesic distances d_G^{ij} computed through the dynamic programming algorithms. The coordinate vectors $x_i \in \vec{X}$ are chosen to minimize the cost function $E = \|\tau(d_G) - \tau(d_X)\|_{L^2}$, where d_X is the matrix of output space distances, d_G is the matrix whose elements are d_G^{ij} and the norm is the matrix L^2 norm $\sqrt{\sum_{i,j} (\tau(d_G) - \tau(d_X))_{ij}^2}$. τ is an operator that converts distances into inner products and is defined as $\frac{1}{2}HSH$, where the centering matrix $H_{ij} = \delta_{ij} - (1/N)$ and the matrix of squared distances $S_{ij} = \left(d_G^{ij}\right)^2$. The global minimum of the cost function is computed by setting the output space coordinates x_i to the top k eigenvectors of $\tau(d_G)$.

E. Practical Implementation

Any feature extraction scheme identifies specific regions in an image that exceed a general information threshold. Each such feature is comprised of several pixels in general, and each pixel can be described by the raw color intensities, multi-scale texture and other visual cues (e.g. intensity gradient, brightness gradient, texture gradient).

In a practical implementation, each extracted feature is subdivided into image patches of a fixed size (e.g. 11×11) and the image patch is described by a single vector of properties of all individual pixels within the patch. These vectors $\vec{Z}$ constitute high dimensional visual observations and form the input to Isomap. Isomap computes a low dimensional representation of high dimensional image patches such that the inherent similarities (or distinctions) in the original patches are preserved. The low dimensional representation physically corresponds to the intrinsic coordinates (or equivalently the visual state) of each patch on the nonlinear manifold.

III. Probabilistic Model

A. The Generative Model

The Isomap algorithm and indeed most NLDR algorithms are inherently *deterministic* algorithms that do not provide a measure of the *uncertainty* of the underlying visual states of high dimensional observations. The integration of the low dimensional states computed by Isomap into a probabilistic, Bayesian filtering framework requires the definition of a generative likelihood model $P(\vec{Z}|\vec{X})$, where $\vec{Z}$ and $\vec{X}$ are the observation and state spaces respectively. This likelihood model encapsulates the uncertainties inherent in the inference of a low dimensional state from noisy high dimensional observations. The incorporation of natural feature states within a non-Gaussian and non-linear filter is expected to significantly enhance data association as the low dimensional appearance states and kinematic variables are complementary.

Methods from supervised learning can be used to derive compact mappings that generalize over large portions of the observation and state space. The input-output pairs of Isomap can serve as training data for an invertible function

approximator in order to learn a parametric mapping between the two spaces.

Given the results of Isomap, a probabilistic model of the joint distribution $P(\vec{Z}, \vec{X})$ can be learnt through the Expectation Maximization (EM) algorithm [6]. The joint distribution can be used to map inputs to outputs and vice versa by computing the expected values $E[\vec{Z}|\vec{X}]$ and $E[\vec{X}|\vec{Z}]$. The joint distribution is represented by a generalization of a mixture of factor analyzers that is termed as a mixture of linear models [14]. The joint distribution is graphically displayed in Figure 1 with the assumed dependencies. The discrete hidden variable s in the model corresponds to a spatial region on the manifold over which a mixture component is representative. This representation conveniently handles highly nonlinear manifolds through the capability to model the local covariance structure of the data in different areas of the manifold.

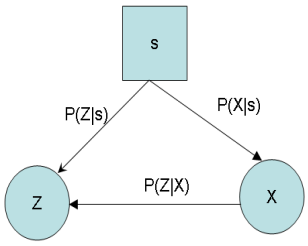

Fig. 1. Graphical model for computation of parametric models from NLDR algorithms. An arrow directed into a node depicts a dependency on the originating node. The discrete hidden variable s represents a specific neighborhood on the manifold.

The complete three step generative model can now be summarized based on the assumed dependencies (Equations 1-3). The joint probability distribution of all the random variables in the graphical model is expressed as

$$P\left(\vec{z}, \vec{x}, s\right) = P(\vec{z} \mid \vec{x}, s)P(\vec{x} \mid s)P\left(s\right) \tag{1}$$

where $\vec{z} \in \vec{Z}$, $\vec{x} \in \vec{X}$ and the dependencies are given by

$$P(\vec{z} \mid \vec{x}, s) = \frac{1}{(2\pi)^{D/2}\left|\Psi_s\right|^{1/2}} \times \tag{2}$$

$$\exp\left\{-\tfrac{1}{2}\left[\vec{z} - \Lambda_s\vec{x} - \mu_s\right]^T \Psi_s^{-1}\left[\vec{z} - \Lambda_s\vec{x} - \mu_s\right]\right\}$$

$$P(\vec{x} \mid s) = \frac{1}{(2\pi)^{d/2}\left|\Sigma_s\right|^{1/2}} \times \tag{3}$$

$$\exp\left\{-\tfrac{1}{2}\left[\vec{x} - \nu_s\right]^T \Sigma_s^{-1}\left[\vec{x} - \nu_s\right]\right\}$$

B. Parameter Estimation

In this model, the set of parameters θ that need to be estimated from the observed high and low dimensional spaces are the prior probabilities $P(s)$, which follow a multinomial distribution, the mean vectors $\vec{\nu_s}$ and $\vec{\mu_s}$, the full covariance matrix Σ_s, the diagonal covariance matrix Ψ_s and the loading matrices Λ_s. The EM algorithm performs iterative parameter estimation by maximizing the log-likelihood of the data given the model and the set of parameters. The observable parameters in the graphical model are denoted as $\{\vec{z}_n, \vec{x}_n\}_{n=1}^N$ where N is the number of samples. EM iteratively maximizes the log-likelihood of the observations

$$\mathcal{L} = \sum_{n=1}^{N} \log \sum_{i=1}^{M} P\left(\vec{z}_n, \vec{x}_n, s_i \mid \theta\right), \tag{4}$$

where M is the number of mixture components considered in the model. Since direct maximization over the above expression is hard to be calculated analytically, an auxiliary distribution $q\left(s_i\right)$ over the hidden variable is introduced:

$$\mathcal{L} = \sum_{n=1}^{N} \log \sum_{i=1}^{M} q\left(s_i\right) \frac{P\left(\vec{z}_n, \vec{x}_n, s_i \mid \theta\right)}{q\left(s_i\right)} \tag{5}$$

Then, it is possible to obtain a lower bound for $\mathcal{L}$ by applying the Jensen's inequality [15]:

$$\mathcal{L} \geq \sum_{n=1}^{N} \log P\left(\vec{z}_n, \vec{x}_n \mid \theta\right) - \tag{6}$$

$$\textstyle\sum_{n=1}^{N}\sum_{i=1}^{M} q\left(s_i\right) \log \frac{q(s_i)}{P(s_i|\vec{z}_n, \vec{x}_n, \theta)}.$$

Thus, maximizing $\mathcal{L}$ with respect to $q\left(s_i\right)$ is equivalent to minimizing the second term of Equation 6, which is the Kullback-Leibler divergence between the free distribution $q\left(s_i\right)$ and the posterior probability $P\left(s_i \mid \vec{z}_n, \vec{x}_n, \theta\right)$.

The update rules for the Maximization step are presented below ([16]):

Defining $\gamma_{sn} = P(s \mid \vec{z}_n, \vec{x}_n)$ and $\omega_{sn} = \frac{\gamma_{sn}}{\sum_{n'} \gamma_{sn'}}$ the updates are:

$$\vec{\nu}_s \leftarrow \sum_n \omega_{sn}\vec{x}_n, \tag{7}$$

$$\Sigma_s \leftarrow \sum_n \omega_{sn}\left[\vec{x}_n - \vec{\nu}_s\right]\left[\vec{x}_n - \vec{\nu}_s\right]^T, \tag{8}$$

$$\Lambda_s \leftarrow \sum_n \omega_{sn}\vec{z}_n\left(\vec{x}_n - \vec{\nu}_s\right)^T \Sigma_s^{-1}, \tag{9}$$

$$\vec{\mu}_s \leftarrow \sum_n \omega_{sn}\left[\vec{z}_n - \Lambda_s\vec{x}_n\right], \tag{10}$$

$$\Psi_s \leftarrow \sum_n \omega_{sn}\left[\vec{z}_n - \Lambda_s\vec{x}_n - \vec{\mu}_s\right]\left[\vec{z}_n - \Lambda_s\vec{x}_n - \vec{\mu}_s\right]^T, \tag{11}$$

$$P(s) \leftarrow \frac{\sum_n \gamma_{sn}}{\sum_{s'n'} \gamma_{s'n'}}. \quad (12)$$

The algorithm continues execution until the difference between the log-likelihood of two iterations is smaller than a given threshold.

C. Comments

Once the parameter estimation is completed, the joint distribution $P(\vec{z}, \vec{x}, s)$ is fully characterized, and a likelihood model $P(\vec{z} = \vec{z_i}|\vec{x})$ (Equation 13) can be computed by making an observation $\vec{z_i}$ in the high dimensional space. Along the lines of the derivation in [14], it can be shown that this likelihood can be expressed as a Gaussian Mixture Model (GMM) that is easily integrated within a non-linear, non-Gaussian filtering scheme [7].

$$P(\vec{z} = \vec{z_i}|\vec{x}) = \sum_s P(s|\vec{z} = \vec{z_i})\, P(\vec{x}|\vec{z_i}, s) \quad (13)$$

IV. Choice of a Suitable Number of Mixture Components

The choice of a specific number of mixture components is crucial to the off-line computation of a likelihood model for high dimensional observations. A rigorous model selection approach has been described in the framework of variational inference [17].

A simpler approach is adopted in this work that adequately addresses over-fitting concerns. The number of mixture components is chosen so that the resulting probabilities $P(s)$ are always greater than a pre-defined threshold. If the computed probabilities $P(s)$ are all significantly greater than the threshold, the model is refined. If any of the mixture components results in probabilities smaller than the threshold, the model is coarsened through a reduction in the number of components.

V. Example Applications

The generative graphical model outlined earlier can be used off-line to compute the model parameters comprised of the means and covariance matrices of the constituent conditional Gaussian distributions. A rigorous approach would necessitate an extensive training set comprised of numerous high dimensional features from representative natural environments that are sampled under realistic ambient conditions.

A. Autonomous Ground Vehicle (AGV) - Inference of Underlying Visual States

A sample of about 9000 high dimensional points physically representing colors and textures of typical objects in the environment such as sky, trees, bush and grass was randomly selected from a sequence of images acquired from a camera mounted on a ground vehicle at the Marulan test facility operated by the Australian Center for Field Robotics. Texture information was included in the high dimensional input space by convolving 11×11 pixel patches with a bank of Gabor wavelets [18] at 2 scales and 2 orientations, resulting in an input space dimensionality of 847. Isomap was used to compute a low dimensional embedding of the training data and the intrinsic dimensionality of the manifold was estimated to be 3. Thus the similarities (or distinctions) in the raw data can be accurately preserved using only 3 dimensions as opposed to 847.

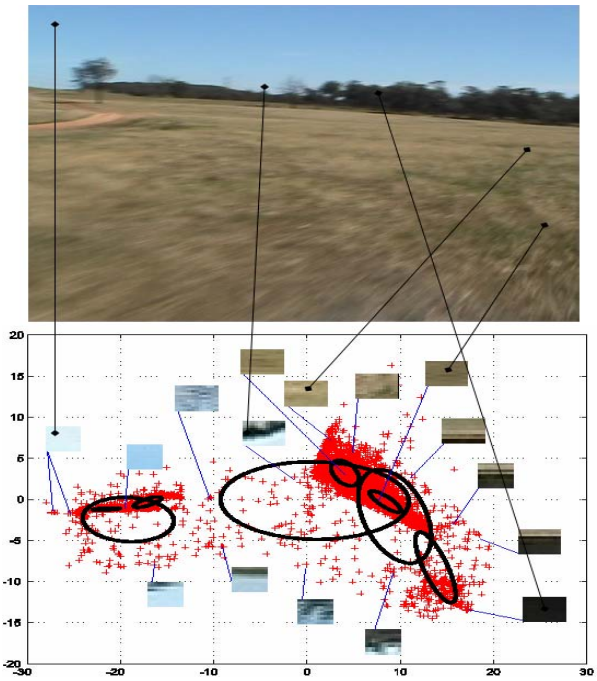

Fig. 2. Sample image acquired by the AGV (**top**) and low dimensional embedding of randomly sampled high dimensional image patches (**bottom**). The learnt low dimensional covariances Σ_s are also overlaid on the plot.

The top two eigenvectors of the computed low dimensional embedding are shown in Figure 2. It is readily observed that image patches corresponding to blue skies are grouped on the left side, those representing bush are on the extreme right, while grass and transitional patches are grouped between the two extremes. The EM algorithm was used to learn the parameters of the generative model (Equations 1-3). The learnt model was subsequently used to infer the low dimensional states (through appropriate marginalization of the joint probability densities) within a typical test image that was acquired in the same environment. The results of inference on the test image (Figure 2 top) in terms of the means of the eigenvectors scaled to gray-scale limits (0-255) for the top two states are shown in Figures 3-4. The different color codes correspond to visually distinct image patches as per their intrinsic location on the manifold.

B. Unmanned Underwater Vehicle (UUV) - Inference of Underlying Visual States

The generality of the feature representation scheme is demonstrated through application in a texture rich underwater environment. A sample of about 17000 high dimensional points physically representing colors and textures of typical objects in an underwater environment such as beach sand and corals was selected from a sequence of images [19] acquired

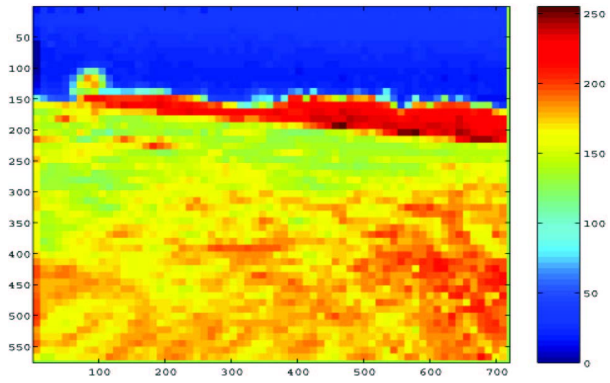

Fig. 3. Contour of the inferred means of the top eigenvector on each 11×11 image patch. This state is correlated to the brightness of the image patches.

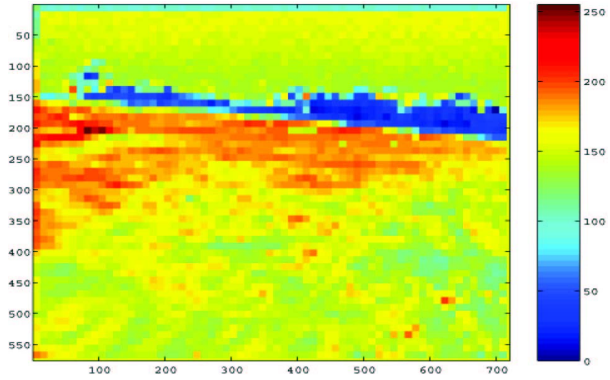

Fig. 4. Contour of inferred means of the second eigenvector. This state allows separation of the bush (range $\approx 0-50$) from the grass and the tracks in the scene.

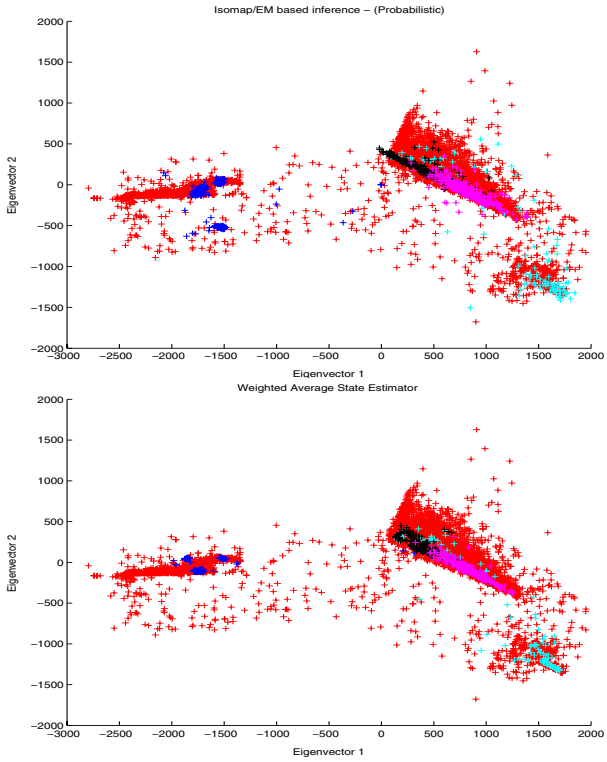

Fig. 5. Inferred low dimensional states (**top**) and weighted average state estimate (**bottom**). The weighted average estimator assumes that the low dimensional state of a test sample is the weighted average of the k nearest high dimensional neighbors of the sample, with the weights being inversely proportional to the high dimensional distances. The trained manifold is represented in red and corresponding test samples are similarly colour coded in each figure.

from a camera mounted onto the UUV Oberon, operated by the Australian Center for Field Robotics.

Isomap and EM were used to compute the probabilistic model off-line, and the learnt model was used to infer the low dimensional states of a typical image acquired by the UUV. The sample image and the results of inference in terms of the fourth eigenvector are shown in Figures 6-7.

C. Comments

Each of the plots depicting the low dimensional states must be interpreted as a contour plot of the respective states in the image plane. It is important to realize that every patch consists of 847 correlated observations in the sensory space, while only a few uncorrelated states are sufficient to capture the similarities (or differences) between the patches after visual state inference.

The inferred low dimensional states are reasonable in that similar high dimensional image patches (such as those corresponding to sky, grass, trees, bush, sand or corals) are assigned similar low dimensional states.

The accuracy of the inferred low dimensional states is qualitatively evaluated in Figures 5 and 8. It is observed from the color coding in these figures that the weighted means of the inferred low dimensional states exhibit good qualitative agreement with a deterministic estimator based on k nearest neighbors. The stochastically inferred estimate is more versatile as it quantifies inherent uncertainties in the inferred states.

VI. Conclusion

The combination of non-parametric manifold learning algorithms with statistical learning strategies leads to a consistent probabilistic description of natural features in unstructured environments. While the entire learning procedure can be incorporated in the training phase of these models that is performed off-line, inference can be performed in *real-time* on any extracted features to compute likelihoods for the natural features as a GMM. Example applications in terrestrial and underwater environments demonstrate the generality and consistency of the representation scheme. Natural features can thus be fully integrated within existing non-Gaussian, non-linear filtering algorithms through the likelihood model so that nonlinear estimation tasks are significantly enhanced through a combination of kinematic and visual states.

Acknowledgment

This work is supported by the ARC Center of Excellence programme, funded by the Australian Research Council (ARC) and the New South Wales (NSW) State Government.

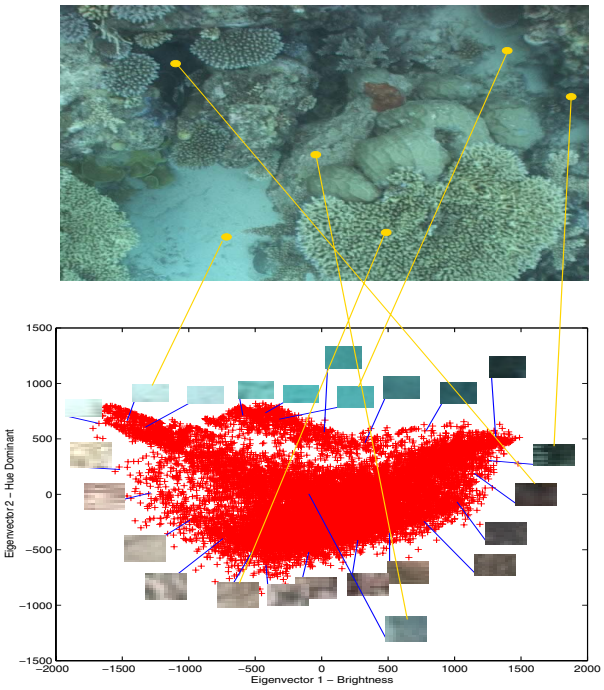

Fig. 6. Sample image acquired by underwater vehicle (top) and low dimensional embedding of randomly sampled image patches (bottom)

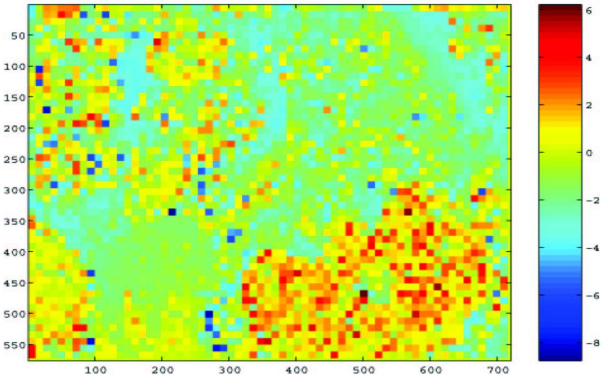

Fig. 7. Inferred means of the fourth eigenvector on each image patch. Distinctions between the sand and the corals are amplified in this state that is correlated to the high frequency texture of the coral colonies.

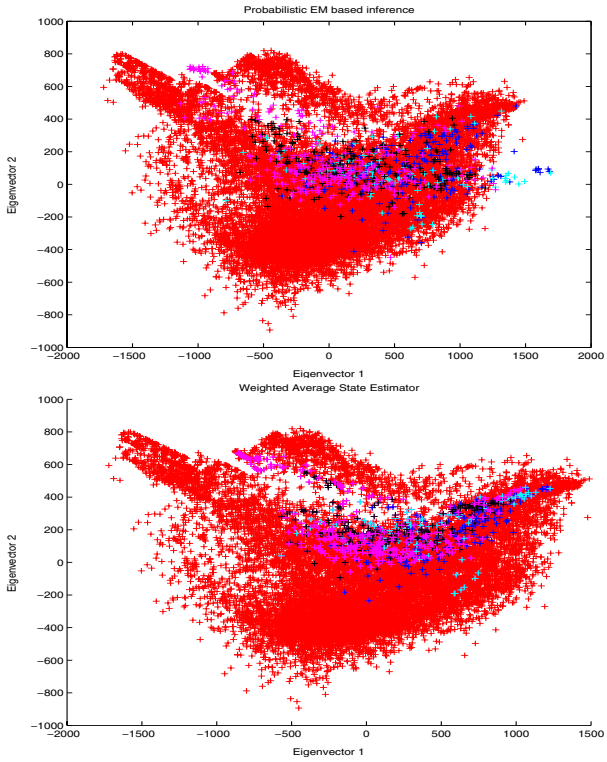

Fig. 8. Inferred low dimensional states (**top**) and weighted average state estimate (**bottom**). The trained manifold is represented in red and corresponding test samples are similarly colour coded in each figure. Good qualitative agreement is observed between the two estimates.

REFERENCES

[1] T. Bailey, *Mobile Robot Localisation and Mapping in Extensive Outdoor Environments*. Ph.D. Dissertation, University of Sydney, 2002.

[2] S. Williams, *Efficient Solutions to Autonomous Navigation and Mapping Problems*. Ph.D. Dissertation, University of Sydney, 2001.

[3] T. Lee, T. Wachtler, and T. J. Sejnowski, "Relations between the statistics of natural images and the response properties of cortical cells," *Vision Research*, vol. 42, pp. 2095–2103, 2002.

[4] Y. Karklin and M. Lewicki, "Learning higher order structure in natural images," *Computation in Neural Systems*, vol. 14, pp. 483–499, 2003.

[5] J. Tenenbaum, V. DeSilva, and J. C. Langford, "A global geometric framework for nonlinear dimensionality redution," *Science*, vol. 290, pp. 2319–2323, 2000.

[6] A. P. Dempster, N. M. Laird, and D. B. Rubin, "Maximum likelihood from incomplete data via the EM algorithm," *Journal of the Royal Statistical Society B*, vol. 39, pp. 1–37, 1977.

[7] B. Upcroft, S. Kumar, M. Ridley, S. Ong, and H. Durrant-Whyte, "Fast Parameter Estimation for General Bayesian Filters in Robotics," in *Proc. Australian Conf. on Robotics and Automation*, 2004.

[8] B. Scholkopf, A. J. Smola, and K. R. Muller, "Nonlinear component analysis as a kernel eigenvalue problem," *Neural Computation*, vol. 10, pp. 1299–1319, 1998.

[9] M. Belkin and P. Niyogi, "Laplacian eigenmaps for dimensionality reduction and data representation," University of Chicago, Department of Computer Science, Tech. Rep., 2002.

[10] S. T. Roweis and L. K. Saul, "Nonlinear dimensionality reduction by Locally Linear Embedding," *Science*, vol. 290, pp. 2323–2326, 2000.

[11] I. Foster, *Designing and Building Parallel Programs*. Addison Wesley, 1995.

[12] E. W. Dijkstra, "A note on two problems in connexion to graphs," *Numerische Mathematik*, vol. 1, pp. 269–271, 1959.

[13] T. Cox and M. Cox, *Multidimensional Scaling*. Chapman and Hall, 1994.

[14] Z. Ghahramani and G. E. Hinton, "The EM algorithm for mixtures of factor analyzers," Department of Computer Science, University of Toronto CRG-TR-96-1, Tech. Rep., 1996.

[15] D. J. MacKay, *Information Theory, Learning and Inference*. Cambridge University Press, 2003.

[16] L. K. Saul and S. T. Roweis, "Think globally, fit locally: Unsupervised learning of nonlinear manifolds," University of Pennsylvania, Department of Computer Science, Tech. Rep., 2002.

[17] M. Beal, *Variational Algorithms for Approximate Bayesian Inference*. Ph.D. Dissertation, University of Cambridge, UK, 1998.

[18] D. J. Field, "Relations between the statistics of natural images and the response properties of cortical cells," *Journal of the Optical Society of America*, vol. 4, pp. 2379–2394, 1987.

[19] S. Williams and I. Mahon, "Simultaneous localization and mapping on the Great Barrier Reef," in *Proc. IEEE Conference on Robotics and Automation*, 2004.